

## Thermodynamic Analysis of $\beta$ -Hairpin-Forming Peptides from the Thermal Dependence of $^1\text{H}$ NMR Chemical Shifts

Clara M. Santiveri, Jorge Santoro, Manuel Rico, and M. Angeles Jiménez\*

Contribution from the Instituto de Química-Física Rocasolano, Consejo Superior de Investigaciones Científicas, Serrano 119, 28006-Madrid, Spain

Received July 25, 2002. Revised Manuscript Received October 14, 2002

**Abstract:** The temperature dependence of the  $^1\text{H}$  chemical shifts of six designed peptides previously shown to adopt  $\beta$ -hairpin structures in aqueous solution has been analyzed in terms of two-state ( $\beta$ -hairpin  $\rightleftharpoons$  coil) equilibrium. The stability of the  $\beta$ -hairpins formed by these peptides, as derived from their  $T_m$  (midpoint transition temperature) values, parallels in general their ability to adopt those structures as deduced from independent NMR parameters: NOEs,  $\Delta\delta_{\text{CaH}}$ ,  $\Delta\delta_{\text{Ca}}$ , and  $\Delta\delta_{\text{C}\beta}$  values. The observed  $T_m$  values are dependent on the particular position within the  $\beta$ -hairpin that is probed, indicating that their folding to a  $\beta$ -hairpin conformation deviates from a "true" two-state transition. To obtain individual  $T_m$  values for each hairpin region in each peptide, a simplified model of a successive uncoupled two-state equilibrium covering the entire process has been applied. The distribution of  $T_m$  values obtained for the different  $\beta$ -hairpin regions (turn, strands, backbone, side chains) in the six analyzed peptides reveals a similar pattern. A model for  $\beta$ -hairpin folding is proposed on the basis of this pattern and the reasonable assumption that regions showing higher  $T_m$  values are the last ones to unfold and, presumably, the first to form. With this assumption, the analysis suggests that turn formation is the first event in  $\beta$ -hairpin folding. This is consistent with previous results on the essential role of the turn sequence in  $\beta$ -hairpin folding.

### Introduction

As a consequence of recent studies on  $\beta$ -hairpin formation by linear peptides, there is now a general consensus on the major factors contributing to their folding and stability (for reviews, see refs 1–7). A quantitative assessment of the contribution of these factors to the stability of  $\beta$ -hairpins in terms of free energies is, however, still lacking. Accurate determination of the folded populations adopted by a  $\beta$ -hairpin-forming peptide and its variants is essential to accomplish this objective. The main problem in determining populations on the basis of NMR parameters is the absence of good reference values for unfolded and especially for completely folded states. Methods commonly used provide only qualitative information on the relative  $\beta$ -hairpin population of related peptides,<sup>8</sup> but they are neither accurate nor precise. Specific models for the unfolded and folded states have been proposed for the particular case of peptides that adopt 2:2  $\beta$ -hairpins and contain a DPro residue at the turn as the main stabilizing factor.<sup>9–11</sup> Also, a method to evaluate  $\beta$ -hairpin stability differences for disulfide-cyclized peptides has

been reported.<sup>12,13</sup> However, there is no general method able to reliably quantify the folded and unfolded populations in  $\beta$ -hairpin conformational equilibrium.

In proteins, the effect of mutations on the free energy of folding can be quantified from the temperature and/or denaturant unfolding curves of the protein and its variants. These unfolding curves are generated by using spectroscopic probes, normally CD and fluorescence. The corresponding unfolding curves in peptides are usually incomplete, because the folded state is hardly ever fully populated at the lowest experimentally accessible temperature as a consequence of the conformational flexibility inherent to linear peptides. This fact hinders the thermodynamic analysis of most peptides. Nevertheless, thermodynamic analyses for the thermal unfolding of a few  $\beta$ -hairpin- and  $\beta$ -sheet-forming peptides have been reported recently.<sup>11,14–22</sup> Many of these analyses use a function of averaged  $\text{C}_\alpha\text{H}$  chemical

\* Corresponding author. Tel: 34-91-5619400. Fax: 34-91-5642431. E-mail: majimenez@iqfr.csic.es.

- (1) Blanco, F. J.; Ramírez-Alvarado, M.; Serrano, L. *Curr. Opin. Struct. Biol.* **1998**, *8*, 107–111.
- (2) Gellman, S. H. *Curr. Opin. Chem. Biol.* **1998**, *2*, 717–725.
- (3) Lacroix, E.; Kortemme, T.; López de la Paz, M.; Serrano, L. *Curr. Opin. Struct. Biol.* **1999**, *9*, 487–493.
- (4) Ramírez-Alvarado, M.; Kortemme, T.; Blanco, F. J.; Serrano, L. *Bioorg. Med. Chem.* **1999**, *7*, 93–103.
- (5) Regan, L. *Curr. Biol.* **1994**, *4*, 656–658.
- (6) Serrano, L. *Adv. Protein Chem.* **2000**, *53*, 49–85.
- (7) Venkatraman, J.; Shankaramma, S. C.; Balaram, P. *Chem. Rev.* **2001**, *101*, 3131–3152.
- (8) Santiveri, C. M.; Rico, M.; Jiménez, M. A. *J. Biomol. NMR* **2001**, *19*, 331–345.

- (9) Syud, F. A.; Espinosa, J. F.; Gellman, S. H. *J. Am. Chem. Soc.* **1999**, *121*, 11578–11579.
- (10) Stanger, H. E.; Syud, F. A.; Espinosa, J. F.; Giriat, I.; Muir, T.; Gellman, S. H. *Proc. Natl. Acad. Sci. U.S.A.* **2001**, *98*, 12015–12020.
- (11) Espinosa, J. F.; Syud, F. A.; Gellman, S. H. *Protein Sci.* **2002**, *11*, 1492–1505.
- (12) Cochran, A. G.; Tong, R. T.; Starovasnik, M. A.; Park, E. J.; McDowell, R. S.; Theaker, J. E.; Skelton, N. J. *J. Am. Chem. Soc.* **2001**, *123*, 625–632.
- (13) Russell, S. J.; Cochran, A. G. *J. Am. Chem. Soc.* **2000**, *122*, 12600–12601.
- (14) Andersen, N. H.; Dyer, R. B.; Fesinmeyer, R. M.; Gai, F.; Liu, Z.; Neidigh, J. W.; Tong, H. *J. Am. Chem. Soc.* **1999**, *121*, 9879–9880.
- (15) Espinosa, J. F.; Gellman, S. H. *Angew. Chem. Int. Ed.* **2000**, *39*, 2330–2333.
- (16) Griffiths-Jones, S. R.; Maynard, A. J.; Searle, M. S. *J. Mol. Biol.* **1999**, *292*, 1051–1069.
- (17) Griffiths-Jones, S. R.; Searle, M. S. *J. Am. Chem. Soc.* **2000**, *122*, 8350–8356.
- (18) Honda, S.; Kobayashi, N.; Muneakata, E. *J. Mol. Biol.* **2000**, *295*, 269–278.

**Table 1.** Peptide Sequences and  $\beta$ -Hairpin Populations Estimated from the  $\delta$ -Values of  $C_{\alpha}H$  Protons and  $^{13}C_{\alpha}$  and  $^{13}C_{\beta}$  Carbons Measured in  $D_2O$  at 5 °C and pH 5.5<sup>8a</sup>

peptide	strand						turn	$\beta$ -hairpin population (%)	
<b>1</b>	S1	Y2	I3	N4	<b>S5</b>		<b>D6</b>	44 ± 4	
		T10	W9	T8	<b>G7</b>				
<b>2</b>	S1	E2	S3	Y4	I5	N6	<b>S7</b>	<b>D8</b>	51 ± 11
	E15	T14	V13	T12	W11	T10	<b>G9</b>		
<b>3</b>	S1	E2	S3	Y4	I5	N6	<b>P7</b>	<b>D8</b>	59 ± 14
	E15	T14	V13	T12	W11	T10	<b>G9</b>		
<b>4</b>	S1	E2	S3	Y4	I5	N6	<b>S7</b>	<b>D8</b>	44 ± 7
	E15	T14	V13	T12	V11	T10	<b>G9</b>		
<b>5</b>	S1	E2	I3	Y4	S5	N6	<b>P7</b>	<b>D8</b>	48 ± 7
	E15	T14	V13	T12	W11	T10	<b>G9</b>		
<b>6</b>	S1	E2	S3	Y4	I5	Y6	<b>N7</b>		31 ± 5
	E14	T13	V12	T11	W10	K9	<b>G8</b>		
<b>7</b>		T1	I2	S3	N4	<b>S5</b>	<b>D6</b>	18 ± 2 <sup>b</sup>	
			T10	W9	T8	<b>G7</b>			

<sup>a</sup> Turn residues are shown in bold. Hydrogen bonds are indicated by vertical lines. Reported errors are the standard deviation. <sup>b</sup>pH 3.7 and 2 °C.

shift values to generate the experimental thermal unfolding curves.<sup>20</sup> By doing so, they do not exploit the main advantage of  $^1H$  chemical shifts relative to other spectroscopic data, namely, that the various  $^1H$  chemical shifts report on different sites along the peptide sequence.

Here, we investigate the temperature dependence of the  $^1H$  chemical shifts of some peptides designed in our group that had been previously demonstrated to adopt significant populations of  $\beta$ -hairpin structures in aqueous solution (peptides **1–6**<sup>8,23–25</sup> in Table 1). In addition, we have examined a seventh peptide that forms a very low population of  $\beta$ -hairpin (peptide **7**<sup>23</sup> in Table 1), as a control for nonstructured peptides. The thermodynamic parameters  $T_m$ ,  $\Delta H_m$ , and  $\Delta S_m$  for the  $\beta$ -hairpin folding of each peptide have been derived from fitting the thermal denaturation curves for all protons displaying significant chemical shift changes and alternatively for subsets of these protons grouped according to their location in the  $\beta$ -hairpin structure: turn, strands, backbone, and side chains. Observation of equal  $T_m$  values for the different subsets of peptide protons would constitute evidence for a two-state  $\beta$ -hairpin–random coil transition, whereas different  $T_m$  values for the various subsets would provide insights into how  $\beta$ -hairpins fold. This second case is the one observed experimentally and permits us to propose a multistep model of  $\beta$ -hairpin folding.

## Materials and Methods

**Peptide Synthesis and Purification.** Peptides **1** and **7** were prepared by solid-phase synthesis and purified by HPLC.<sup>23</sup> Peptides **2**, **3**, and **5** were provided by the Servei de Síntesi at the Department of Organic Chemistry (University of Barcelona, Spain), and peptides **4** and **6** were acquired from DiverDrugs (Barcelona, Spain).

**NMR.** Samples for NMR experiments were prepared in 0.5 mL of pure  $D_2O$  or  $H_2O/D_2O$  9:1 v/v at 1–5 mM peptide concentrations. The pH was measured with a glass microelectrode and was not corrected for isotope effects. The temperature of the NMR probe was calibrated using a methanol sample. Sodium [3-trimethylsilyl-2,2,3,3- $^2H_4$ ]propionate (TSP) was used as an internal reference. The  $^1H$  NMR spectra were acquired on a Bruker AMX-600 pulse spectrometer operating at a  $^1H$  frequency of 600.13 MHz. 1D spectra were acquired using 32K data points, which were zero-filled to 64K data points before performing the Fourier transformation. Total correlated spectroscopy (TOCSY<sup>26</sup>) spectra were recorded by standard techniques using presaturation of the water signal in the time-proportional phase incrementation mode<sup>27</sup> and a 80 ms MLEV17 with  $z$  filter spin-lock sequence.<sup>26</sup> Acquisition data matrixes were defined by 2048 × 512 points in  $t_2$  and  $t_1$ , respectively. Data were processed using the standard XWIN NMR Bruker program on a Silicon Graphics computer. The 2D data matrix was multiplied by a square–sine–bell window function with the corresponding shift optimized for every spectrum and zero-filled to a 2K × 1K complex matrix prior to Fourier transformation. Baseline correction was applied in both dimensions.

The thermal dependence of  $^1H$  chemical shifts of peptides **1–6** in  $D_2O$  at pH 5.5 and peptide **7** in  $D_2O$  at pH 3.7 was measured by a series of 1D and 2D TOCSY spectra acquired at 2, 5, and 10 °C intervals over the range of –4 to 80 °C. The same protocol was used for peptide **2** in 2 M NaCl and 2 M Gly and for peptide **5** in 30% TFE, except the temperature range was –15 to 80 °C for peptide **2** in 2 M NaCl and –10 to 70 °C for peptide **5** in 30% TFE.

**Estimation of  $\beta$ -Hairpin Populations.** Independent determinations of  $\beta$ -hairpin populations were performed for each peptide from the conformational shifts  $\Delta\delta_{CaH}$  ( $\delta_{CaH}(\text{observed}) - \delta_{CaH}(\text{random coil})$ , ppm),  $\Delta\delta_{Ca}$  ( $\delta_{Ca}(\text{observed}) - \delta_{Ca}(\text{random coil})$ , ppm), and  $\Delta\delta_{C\beta}$  ( $\delta_{C\beta}(\text{observed}) - \delta_{C\beta}(\text{random coil})$ , ppm) averaged over the strand residues, excluding the N- and C-terminal residues and those with anomalous  $\Delta\delta_{CaH}$ ,  $\Delta\delta_{Ca}$ , or  $\Delta\delta_{C\beta}$  values. Null or positive  $\Delta\delta_{Ca}$  values and null or negative  $\Delta\delta_{CaH}$  and  $\Delta\delta_{C\beta}$  values were considered to be anomalous, since negative and positive values are characteristic of  $\beta$ -strands.<sup>8</sup> The reference values for  $C_{\alpha}H$  chemical shifts of each residue in the random coil state were taken from the work of Bundi and Wüthrich,<sup>28</sup> and those for  $^{13}C_{\alpha}$  and  $^{13}C_{\beta}$  chemical shifts were from Wishart et al.<sup>29</sup> Since these  $^{13}C$   $\delta$  values are referenced to DSS and peptides **1–7** to TSP, the corresponding correction was applied ( $\approx 0.1$  ppm<sup>30</sup>). The reference values for 100%  $\beta$ -hairpin were the mean conformational shifts reported for protein  $\beta$ -sheets: 0.40 ppm for  $\Delta\delta_{CaH}$ ,<sup>31</sup> –1.6 ppm for  $\Delta\delta_{Ca}$ ,<sup>8</sup> and 1.7 ppm for  $\Delta\delta_{C\beta}$ .<sup>8</sup>

**Thermodynamic Analysis.** In a fast equilibrium between two states, such as the folding and unfolding of peptides **1–7**, the chemical shift observed for each peptide proton is the weighted average of the  $\delta$  values corresponding to the unfolded state,  $\delta_U$ , and to the  $\beta$ -hairpin structure,  $\delta_F$ ,

$$\delta^{\text{obs}}(T) = \delta_U (1 - \chi_F(T)) + \delta_F \chi_F(T) = \delta_U + \chi_F(T) \Delta\delta \quad (1)$$

where  $\chi_F$  is the mole fraction of the peptide in the folded  $\beta$ -hairpin

(19) Kobayashi, N.; Honda, S.; Yoshii, H.; Munekata, E. *Biochemistry* **2000**, *39*, 6564–6571.

(20) Maynard, A. J.; Sharman, G. J.; Searle, M. S. *J. Am. Chem. Soc.* **1998**, *120*, 1996–2007.

(21) Searle, M. S.; Griffiths-Jones, S. R.; Skinner-Smith, H. *J. Am. Chem. Soc.* **1999**, *121*, 11615–11620.

(22) Sharman, G. J.; Searle, M. S. *J. Am. Chem. Soc.* **1998**, *120*, 5291–5300.

(23) de Alba, E.; Rico, M.; Jiménez, M. A. *Protein Sci.* **1997**, *6*, 2548–2560.

(24) de Alba, E.; Rico, M.; Jiménez, M. A. *Protein Sci.* **1999**, *8*, 2234–2244.

(25) Santiveri, C. M.; Rico, M.; Jiménez, M. A. *Protein Sci.* **2000**, *9*, 2151–2160.

(26) Rance, M. J. *Magn. Reson.* **1987**, *74*, 557–564.

(27) Redfield, A. G.; Kuntz, S. D. *J. Magn. Reson.* **1975**, *19*, 250–259.

(28) Bundi, A.; Wüthrich, K. *Biopolymers* **1979**, *18*, 285–297.

(29) Wishart, D. S.; Bigam, C. G.; Holm, A.; Hodges, R. S.; Sykes, B. D. *J. Biomol. NMR* **1995**, *5*, 67–81.

(30) Wishart, D. S.; Bigam, C. G.; Yao, J.; Abildgaard, F.; Dyson, H. J.; Oldfield, E.; Markley, J. L.; Sykes, B. D. *J. Biomol. NMR* **1995**, *6*, 135–140.

(31) Wishart, D. S.; Sykes, B. D.; Richards, F. M. *J. Mol. Biol.* **1991**, *222*, 311–333.

structure, and  $\Delta\delta = \delta_F - \delta_U$ .  $\delta_U$  and  $\delta_F$  are considered temperature-independent. This assumption is reasonable, since chemical shifts for nonexchangeable protons in nonstructured peptides are practically unaffected by temperature.<sup>32–34</sup> Fitting the experimental melting curves to this equation yields values for  $\delta_U$  and  $\Delta\delta$  as well as for the temperature of the transition midpoint,  $T_m$ , and the enthalpy and heat capacity changes for unfolding,  $\Delta H_m$  and  $\Delta C_p$ , respectively, using the thermodynamic expressions established by Privalov and co-workers.<sup>35</sup>  $\Delta C_p$  is assumed to be temperature independent.

A Fortran program was written to simultaneously fit multiple thermal denaturation curves. The fitting procedure was simplified by splitting it into two steps, one linear and the other nonlinear, with  $\Delta H_m$ ,  $T_m$ , and  $\Delta C_p$  being the only parameters considered in the nonlinear step. For each set of thermodynamic parameters, a value for  $\chi_F(T)$  is calculated first and then used to obtain values for  $\delta_U$  and  $\Delta\delta$  for each proton by linear least-squares fitting of eq 1.

Once the  $\delta_U$  and  $\Delta\delta$  values are calculated, application of eq 1 yields the  $\delta^{\text{cal}}(T)$  corresponding to the trial set of thermodynamic parameters. The best  $\Delta H_m$ ,  $T_m$ , and  $\Delta C_p$  values are those for which the  $\chi^2$  function is minimal:

$$\chi^2 = \sum_i \sum_j \left[ \frac{\delta_i^{\text{obs}}(T_j) - \delta_i^{\text{cal}}(T_j)}{\sigma} \right]^2 \quad (2)$$

where  $\sigma$  is the error in the chemical shift measurement considered to be 0.01 ppm for all protons at all temperatures. Subindices  $i$  and  $j$  refer to the kind of proton and to the temperature, respectively. The program uses the simplex method<sup>36</sup> to minimize the  $\chi^2$  function or alternatively scans systematically the thermodynamic parameters. The fitting procedure used has the advantages of a drastic reduction in the number of variables involved in the nonlinear fitting, which greatly increases the calculation speed.

When  $\Delta C_p$  is assumed to be 0, a contour plot of  $\chi^2$  can be generated for various values of  $\Delta H_m$  and  $T_m$  to obtain the confidence limits of these thermodynamic parameters.

**Estimation of Polar ( $\Delta\text{ASA}_{\text{polar}}$ ) and Nonpolar ( $\Delta\text{ASA}_{\text{nonpolar}}$ ) Surface Areas Buried upon  $\beta$ -Hairpin Formation.** The solvent-accessible polar and nonpolar areas for the structures formed by all peptides were calculated using the program VADAR.<sup>37</sup> The polar and nonpolar surface areas buried upon  $\beta$ -hairpin formation were computed, respectively, as the differences between the solvent-accessible polar and nonpolar areas averaged over the 20 best calculated structures<sup>23–25,38</sup> and the corresponding areas in a completely extended peptide.

## Results

**Temperature Dependence of  $^1\text{H}$  Chemical Shifts of Peptides 1–7.** The temperature variation of  $^1\text{H}$  chemical shifts of all protons of peptides 1–6 in  $\text{D}_2\text{O}$  at pH 5.5 and of peptide 7 at pH 3.7 (Table 1) was followed by assignment of their 2D TOCSY spectra recorded at temperatures ranging from  $-4$  to  $80$  °C. To better define the native state pretransition baseline, additional experiments were performed using cosolutes to enhance the stability of the  $\beta$ -hairpin conformation, namely,

peptide 2 in 2 M Gly<sup>39,40</sup> and peptide 5 in 30% TFE,<sup>20,24,41–45</sup> or to decrease the freezing point, namely, peptide 2 in 2 M NaCl.

In the temperature range studied, all peptide 7 protons show very small chemical shift changes [ $|\Delta\delta_{(T,\text{low}-T,\text{high})}| < 0.10$  ppm, where  $\Delta\delta_{(T,\text{low}-T,\text{high})} = \delta_{T,\text{low}} - \delta_{T,\text{high}}$  (ppm), with  $\delta_{T,\text{low}}$  and  $\delta_{T,\text{high}}$  being the  $^1\text{H}$  chemical shifts measured at the lowest and highest temperature, respectively] with an approximately linear temperature dependence, as seen in the case of the  $\text{C}_\alpha\text{H}$  protons shown in Figure 1. This was the expected behavior, since this peptide is largely unfolded (Table 1) and since changes in the chemical shift of protons in model random coil peptides over the entire temperature range are minimal (ca. 0.02 ppm over  $40$  °C).<sup>34</sup>

In contrast to peptide 7, the total  $|\Delta\delta_{(T,\text{low}-T,\text{high})}|$  values for many protons in peptides 1–6 are much larger ( $|\Delta\delta_{(T,\text{low}-T,\text{high})}| > 0.30$  ppm and even  $> 0.75$  ppm in some cases) under all solvent conditions examined. Moreover, the  $\delta$  values for most of these protons display a broad sigmoidal temperature dependence, as can be appreciated in the  $\delta$  vs  $T$  plots for the  $\text{C}_\alpha\text{H}$  protons of peptides 1, 2, and 5 (Figures 1 and 2). As expected, the plateau corresponding to the folded  $\beta$ -hairpin structure is better defined in the  $\delta$  vs  $T$  curves of peptide 5 in 30% TFE than in  $\text{D}_2\text{O}$ , but transitions are not complete, because the peptide is not fully unfolded in 30% TFE at the highest temperature recorded,  $70$  °C. This is clearly seen in the case of the  $\text{C}_\alpha\text{H}$  protons shown in Figure 1. Regarding the effect of either 2 M NaCl or 2 M Gly, contrary to our expectations, both agents slightly decrease the  $\beta$ -hairpin population adopted by peptide 2 (see the Supporting Information), and as a consequence, the folded-state plateau displayed by the thermal unfolding curves of peptide 2 in the presence of either of these agents is worse defined than in  $\text{D}_2\text{O}$ .

Despite the uncertainty in the folded and unfolded baselines, the transitions of peptides 1–6 were judged as amenable to a quantitative thermodynamic analysis.

**Thermodynamic Analysis of Peptides 1–6.** Values for the thermodynamic parameters  $T_m$ ,  $\Delta H_m$ , and  $\Delta C_p$  of the  $\beta$ -hairpin conformational equilibrium in peptides 1–6 were determined from a fitting of  $\delta$  vs  $T$  curves, by assuming a two-state transition (see Materials and Methods). Protons with  $|\Delta\delta_{(T,\text{low}-T,\text{high})}| \leq 0.10$  were excluded from the fitting, though those with  $|\Delta\delta_{(T,\text{low}-T,\text{high})}| \geq 0.06$  ppm were included if the equivalent proton in some other peptide fulfills the condition  $|\Delta\delta_{(T,\text{low}-T,\text{high})}| > 0.10$  ppm (for example,  $\text{C}_\alpha\text{H}$  of N6 in peptide 3 and  $\text{C}_\alpha\text{H}$  of E2 in peptide 6). These limits were considered reasonable on the basis of the behavior reported for model unfolded peptides<sup>34</sup> and observed for peptide 7 (see the previous section).

Fits performed fixing  $\Delta C_p \neq 0$  led to very low  $\Delta C_p$  values and to very large errors for  $T_m$ ,  $\Delta H_m$ , and  $\Delta C_p$ . Since analysis of thermal denaturation of peptides typically yields large uncertainties in  $\Delta C_p$ , especially if their values are small,<sup>14</sup> we assumed  $\Delta C_p = 0$  for all the fits reported here. This assumption

- (32) Nieto, J. L.; Rico, M.; Santoro, J.; Herranz, J.; Bermejo, F. J. *Int. J. Pept. Protein Res.* **1986**, *28*, 315–323.  
 (33) Peña, M. C.; Rico, M.; Jiménez, M. A.; Herranz, J.; Santoro, J.; Nieto, J. L. *Biochim. Biophys. Acta* **1988**, *957*, 380–389.  
 (34) Merutka, G.; Dyson, H. J.; Wright, P. E. *J. Biomol. NMR* **1995**, *5*, 14–24.  
 (35) Privalov, P. L. *Adv. Protein Chem.* **1979**, *33*, 167–241.  
 (36) Press, W. H.; Vetterling, W. T.; Teukolsky, S. A.; Flannery, B. P. *Numerical recipes in Fortran. The art of scientific computing*; Cambridge University Press: Cambridge, 1992.  
 (37) Wishart, D. S.; Willard, L.; Sykes, B. D. *VADAR. Volume angles defines area, version 1.3*; University of Alberta. Protein Engineering Network of Centres of Excellence: Edmonton, 1996.  
 (38) Santiveri, C. M. In *Facultad de Ciencias Químicas*; Universidad Complutense de Madrid: Madrid, Spain, 2002.

- (39) Foord, R. L.; Leatherbarrow, R. J. *Biochemistry* **1998**, *37*, 2969–2978.  
 (40) Matthews, S. J.; Leatherbarrow, R. J. *J. Biomol. NMR* **1993**, *3*, 597–600.  
 (41) Buck, M. Q. *Rev. Biophys.* **1998**, *31*, 297–355.  
 (42) Blanco, F. J.; Serrano, L. *Eur. J. Biochem.* **1995**, *230*, 634–649.  
 (43) de Alba, E.; Jiménez, M. A.; Rico, M.; Nieto, J. L. *Fold Des.* **1996**, *1*, 133–144.  
 (44) Ramírez-Alvarado, M.; Blanco, F. J.; Serrano, L. *Nat. Struct. Biol.* **1996**, *3*, 604–612.  
 (45) Ramírez-Alvarado, M.; Blanco, F. J.; Niemann, H.; Serrano, L. *J. Mol. Biol.* **1997**, *273*, 898–912.

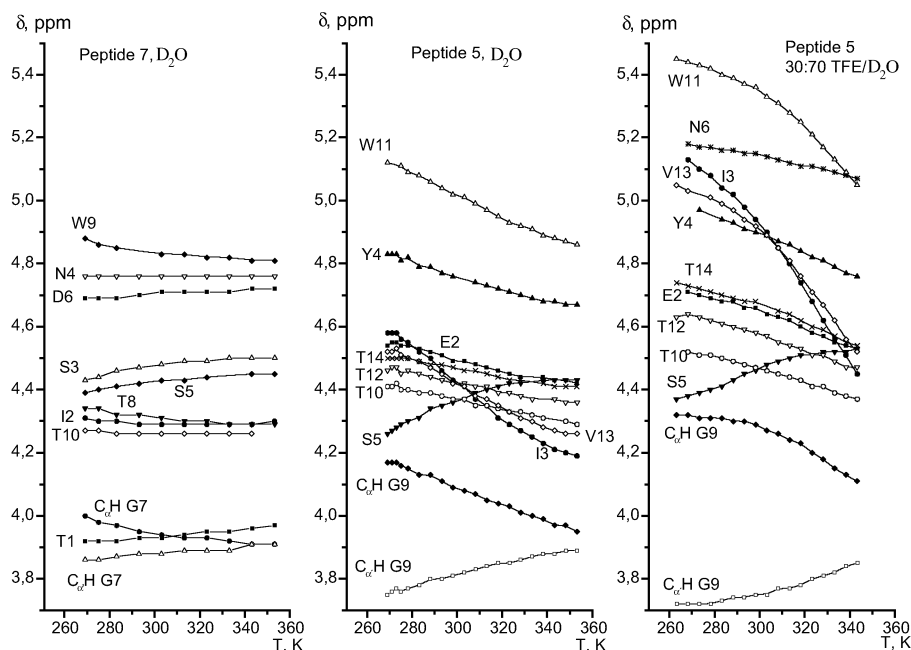


**Figure 1.**  $\delta$ -Values of the  $C_{\alpha}H$  protons of peptide **7** in  $D_2O$  at pH 3.7 and of peptide **5** in  $D_2O$  and 30% TFE at pH 5.5 as a function of temperature. Experimental points are linked with a line to guide the eye.

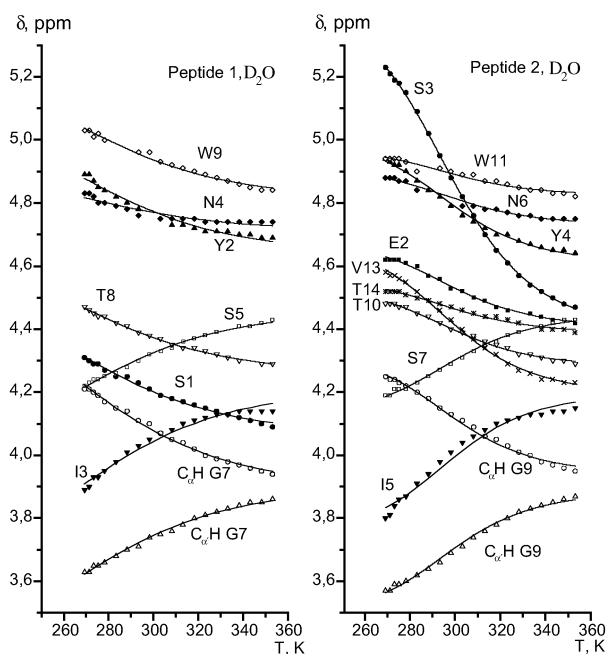


**Figure 2.**  $\delta$ -Values of the  $C_{\alpha}H$  protons of peptides **1** and **2** in  $D_2O$  at pH 5.5 as a function of temperature. The symbols represent the experimental points. The line resulting from fitting to eq 1 is also plotted.

is commonly adopted in studies on  $\alpha$ -helix<sup>46,47</sup> and  $\beta$ -sheet<sup>18,19,22,48</sup> folding. Representative fits are shown in Figure 2. The  $T_m$  and  $\Delta H_m$  values obtained for peptides **1–6** in this way as well as their  $\Delta S_m$  values are listed in Table 2. Fitting the  $\delta$  vs  $T$  curves of peptide **7** protons with  $|\Delta\delta_{(T_{low}-T_{high})}| > 0.06$  ppm led to completely undetermined  $T_m$  and  $\Delta H_m$  values, as expected from their approximately linear appearance (Figure 1).

**Table 2.**  $T_m$  and  $\Delta H_m$  Values for  $\beta$ -Hairpin Unfolding in Peptides **1–6** at pH 5.5 for Protons with  $|\Delta\delta_{(T_{low}-T_{high})}| > 0.10$  ppm<sup>a</sup>

peptide, solvent	number of protons	$T_m$ (K)	$\Delta H_m$ (kJ mol <sup>-1</sup> )	$\Delta S_m$ (J K <sup>-1</sup> mol <sup>-1</sup> )
<b>1</b> , $D_2O$	26	285.2 $\pm$ 0.1	30.8 $\pm$ 0.2	108.0 $\pm$ 0.7
<b>2</b> , $D_2O$	29	296.9 $\pm$ 0.1	39.4 $\pm$ 0.2	132.6 $\pm$ 0.6
<b>2</b> , 2 M NaCl	29	286.2 $\pm$ 0.1	34.3 $\pm$ 0.2	119.7 $\pm$ 0.7
<b>2</b> , 2 M Gly	29	297.6 $\pm$ 0.2	38.5 $\pm$ 0.3	129.3 $\pm$ 1.1
<b>3</b> , $D_2O$	28	304.1 $\pm$ 0.1	35.1 $\pm$ 0.2	115.5 $\pm$ 0.5
<b>4</b> , $D_2O$	19	299.0 $\pm$ 0.2	28.0 $\pm$ 0.2	93.7 $\pm$ 0.8
<b>5</b> , $D_2O$	22	305.2 $\pm$ 0.2	28.2 $\pm$ 0.2	92.3 $\pm$ 0.8
<b>5</b> , 30% TFE	24	345.6 $\pm$ 0.3	30.1 $\pm$ 0.2	87.1 $\pm$ 0.7
<b>6</b> , $D_2O$	19	287.4 $\pm$ 0.2	30.7 $\pm$ 0.3	106.9 $\pm$ 1.1

<sup>a</sup>  $\Delta S_m$  values were obtained from  $\Delta H_m$  and  $T_m$  considering that the free energy of unfolding is null at the transition midpoint. Errors for  $\Delta H_m$  and  $T_m$  were estimated from the variance-covariance matrix and those for  $\Delta S_m$  by error propagation.

Apart from the fittings performed simultaneously for all  $\delta$  vs  $T$  curves corresponding to protons with significant  $\Delta\delta_{(T_{low}-T_{high})}$  (see above), independent fittings were performed for four subgroups of these protons. The subgroups were formed by classifying the protons according to their location in the  $\beta$ -hairpin structure, i.e., protons belonging to residues at the turn and at the strands. Protons located in strands were additionally subdivided into backbone and side chain protons. The equivalent subdivision was not applied to protons belonging to the turn because of their small number (three to six in total, depending on the peptide). The  $T_m$  values obtained for the four considered subsets in peptides **1–6** are listed in Table 3.

## Discussion

The thermodynamic parameters  $T_m$ ,  $\Delta H_m$ , and  $\Delta S_m$ , of the folding–unfolding equilibrium of a series of  $\beta$ -hairpin-forming peptides have been obtained on the basis of the temperature dependence of  $^1H$  chemical shifts. The higher the  $\beta$ -hairpin populations adopted by the peptides, the better the  $T_m$  and  $\Delta H_m$  values obtained from a fitting of their  $\delta$  vs  $T$  curves.

- (46) Rico, M.; Santoro, J.; Bermejo, F. J.; Herranz, J.; Nieto, J. L.; Gallego, E.; Jimenez, M. A. *Biopolymers* **1986**, *25*, 1031–1053.  
 (47) Huang, C.-Y.; Klemke, J. W.; Getahun, Z.; DeGrado, W. F.; Gai, F. J. *Am. Chem. Soc.* **2001**, *123*, 9235–9238.  
 (48) Honda, S.; Kobayashi, N.; Munekata, E.; Uedaira, H. *Biochemistry* **1999**, *38*, 1203–1213.

**Table 3.**  $T_m$  (K) Values for  $\beta$ -Hairpin Unfolding Obtained from the Fitting of the  $\delta$  vs  $T$  Curves of Peptides 1–6 at pH 5.5 for Protons with  $|\Delta\delta(\tau_{low}-\tau_{high})| > 0.10$  ppm Located in the Turn Region and at the Strands<sup>a</sup>

peptide	solvent	turn	strands		
			all	backbone	side chain
<b>1</b>	D <sub>2</sub> O	<b>294.3 ± 0.4</b>	284.7 ± 0.1	<i>b</i>	286.2 ± 0.1
<b>2</b>	D <sub>2</sub> O	<b>305.1 ± 0.3</b>	296.3 ± 0.1	296.8 ± 0.2	296.1 ± 0.1
<b>2</b>	2 M NaCl	<b>291.2 ± 0.4</b>	285.9 ± 0.1	286.5 ± 0.2	285.7 ± 0.1
<b>2</b>	2 M Gly	<b>300.2 ± 0.5</b>	297.3 ± 0.2	284.6 ± 0.4	298.6 ± 0.2
<b>3</b>	D <sub>2</sub> O	<b>316.2 ± 0.3</b>	303.2 ± 0.1	302.9 ± 0.2	303.4 ± 0.1
<b>4</b>	D <sub>2</sub> O	<b>305.3 ± 0.4</b>	296.8 ± 0.2	292.2 ± 0.3	304.5 ± 0.4
<b>5</b>	D <sub>2</sub> O	<b>310.4 ± 0.5</b>	304.7 ± 0.2	304.8 ± 0.3	304.6 ± 0.3
<b>5</b>	30% TFE	337.7 ± 0.6	346.8 ± 0.3	<b>347.7 ± 0.3</b>	342.9 ± 0.5
<b>6</b>	D <sub>2</sub> O	<b>291.0 ± 0.5</b>	286.9 ± 0.2	<b>291.5 ± 0.4</b>	284.2 ± 0.3

<sup>a</sup> Strand protons were subsequently subdivided into backbone and side chain protons. The highest  $T_m$  value for each peptide is shown in bold. Errors were estimated from the variance-covariance matrix. <sup>b</sup> Analysis of  $\chi^2$  contour maps (Materials and Methods) indicated that  $T_m$  cannot be determined accurately for this group of protons.

**Enthalpic and Entropic Contributions to  $\beta$ -Hairpin Unfolding.** The positive sign of  $\beta$ -hairpin unfolding  $\Delta H_m$  and  $\Delta S_m$  values in peptides 1–6 (Table 2) indicates that  $\beta$ -hairpin formation is enthalpy-favored and entropy-disfavored. This suggests that van der Waals and electrostatic interactions, including hydrogen bonds, contribute more to  $\beta$ -hairpin stability than the solvent-related hydrophobic effect.<sup>20</sup> Similar behavior has been reported for the 41–56 fragment from the B1 domain of protein G and some of its variants,<sup>18,19</sup> as well as for some designed DPro-containing peptides<sup>11,15</sup> in aqueous solution. In contrast, a designed 16-residue peptide was reported to have negative unfolding  $\Delta H^\circ$  and  $\Delta S^\circ$  values in aqueous solution and in 8% HFIP, although they were positive in the presence of methanol, TFE, and 20% HFIP, showing that  $\beta$ -hairpin folding is entropy-driven with the hydrophobic effect as the main force contributing to it.<sup>14,20</sup>

Regarding  $\Delta C_p$ , a very low or null value is considered indicative of a small hydrophobic contribution to the stability of the protein or peptide structure. This is the case for  $\beta$ -hairpin stability in peptides 1–6, for which satisfactory  $\delta$  vs  $T$  curve fittings can be obtained by assuming  $\Delta C_p = 0$ . If, alternatively, we assume  $\Delta C_p \neq 0$ , the resulting  $\Delta C_p$  values, though showing a large error, are very low indeed. We have determined the  $\Delta ASA_{nonpolar}$ , i.e., the hydrophobic surface buried upon folding. No correlation was found between that value and the stability of the formed  $\beta$ -hairpin at low temperature (5 °C), which is in agreement with a small hydrophobic contribution to  $\beta$ -hairpin stability. Differences in  $\Delta ASA_{nonpolar}$  per residue among the investigated peptides here are very small. The null  $\Delta C_p$  values reported for  $\beta$ -hairpin unfolding in other peptides<sup>18,19,22,48</sup> are in accord with the results found here for peptides 1–6. Only the 16-residue  $\beta$ -hairpin peptide under the solvent conditions where it shows negative signs for the unfolding  $\Delta H^\circ$  and  $\Delta S^\circ$  values displays large  $\Delta C_p$  values (1400 J K<sup>-1</sup> mol<sup>-1</sup> in water<sup>20</sup> and 1730 J K<sup>-1</sup> mol<sup>-1</sup> in 8% HFIP<sup>14</sup>). The magnitude of the hydrophobic contribution to  $\beta$ -hairpin stability appears to depend on peptide sequence and solvent conditions.

**Comparison of  $\beta$ -Hairpin Formation in Peptides 1–6 Based on  $T_m$  Values.** The relative stability of the  $\beta$ -hairpin structures adopted by peptides 1–6 in aqueous solution shall be compared on the basis of their  $T_m$  values, since  $T_m$  is the most precisely determined parameter from the unfolding curve

fittings. In general, peptides with the most populated  $\beta$ -hairpins have the highest  $T_m$  values; that is, their  $\beta$ -hairpin structures unfold at higher temperature. Indeed, there is a strong relationship between the  $\beta$ -hairpin populations and the  $T_m$  values, as indicated by the  $r$  value (0.97) for the correlation between the  $\beta$ -hairpin populations estimated at 25 °C<sup>38</sup> and the  $T_m$  values obtained from fitting the unfolding curves for peptides 2–6 (Table 2), including data for peptide 2 in 2 M NaCl and in 2 M Gly and for peptide 5 in 30% TFE. Despite incomplete denaturation curves for peptide 6, the  $T_m$  values reflect the lower stability of the peptide 6  $\beta$ -hairpin relative to those of peptides 2 and 3 (Tables 1 and 2). The cases where  $T_m$  values do not exactly conform to the  $\beta$ -hairpin stability order derived from the estimated populations, such as the peptide pairs 2 and 4, and 3 and 5 (Tables 1 and 2), may be due to small differences in the actual values of  $\Delta H_m$  and  $\Delta S_m$ , which can make the curves either sharper or broader. Apart from this, the correlation between the relative  $\beta$ -hairpin stability deduced from  $T_m$  values and from the populations estimated from  $C_{\alpha H}$ ,  $^{13}C_{\alpha}$ , and  $^{13}C_{\beta}$   $\delta$  values is excellent.

On the basis of the order of  $\beta$ -hairpin stability obtained for peptides 1–6, we examined several factors contributing to  $\beta$ -hairpin formation. Since the 3:5  $\beta$ -hairpins formed by peptides 1 and 2 differ only in that the strands of peptide 2 are longer, its higher stability is evidence that strand length contributes to  $\beta$ -hairpin formation, as has been reported for 2:2  $\beta$ -hairpin-forming peptides.<sup>10</sup> The increased  $\beta$ -hairpin stability of peptides 3 compared to peptide 2 is in good agreement with the statistical preference for P (peptide 3) over S (peptide 2) at position  $i + 1$  in a type I  $\beta$ -turn (position 7 in peptides 2 and 3; Table 1<sup>49</sup>). This confirms the important role of the turn sequence for  $\beta$ -hairpin stability.<sup>12,23,24,43,45,50–54</sup>

Concerning the destabilizing effect of salt on the peptide 2  $\beta$ -hairpin (Table 2), one must consider that salts, in addition to lowering the freezing point, screen electrostatic interactions, which could lower the  $\beta$ -hairpin population, as occurs in some  $\alpha$ -helical peptides.<sup>55,56</sup> This peptide contains two electrostatic interactions which have been demonstrated to contribute to the stability of  $\beta$ -hairpins,<sup>43,57</sup> namely, between the oppositely charged N- and C-termini and between the N6 side chain amide and D8 carboxylate groups in the turn. On the other hand, the stabilizing effect of TFE on  $\beta$ -hairpin formation is confirmed in peptide 5 by the drastic  $T_m$  increase of 40 °C (Table 2).

**$\beta$ -Hairpin-Folding Model.** In most of the peptides, the  $T_m$  values obtained from all protons with significant  $|\Delta\delta(\tau_{low}-\tau_{high})|$  (see Results) and from subsets of protons from different peptide regions show some differences (Table 3). These discrepancies indicate that the  $\beta$ -hairpin to unfolded state transition for the whole peptide molecule deviates from a global two-state model. At this point it is convenient to make some clarifying remarks.

- (49) Hutchinson, E. G.; Thornton, J. M. *Protein Sci.* **1994**, *3*, 2207–2216.  
 (50) Searle, M. S.; Williams, D. H.; Packman, L. C. *Nat. Struct. Biol.* **1995**, *2*, 999–1006.  
 (51) de Alba, E.; Jiménez, M. A.; Rico, M. *J. Am. Chem. Soc.* **1997**, *119*, 175–183.  
 (52) Haque, T. S.; Gellman, S. H. *J. Am. Chem. Soc.* **1997**, *119*, 2303–2304.  
 (53) Stanger, H. E.; Gellman, S. H. *J. Am. Chem. Soc.* **1998**, *120*, 4236–4237.  
 (54) Chen, P. Y.; Lin, C. K.; Lee, C. T.; Jan, H.; Chan, S. I. *Protein Sci.* **2001**, *10*, 1794–1800.  
 (55) Fairman, R.; Shoemaker, K. R.; York, E. J.; Stewart, J. M.; Baldwin, R. L. *Proteins* **1989**, *5*, 1–7.  
 (56) Fairman, R.; Shoemaker, K. R.; York, E. J.; Stewart, J. M.; Baldwin, R. L. *Biophys. Chem.* **1990**, *37*, 107–119.  
 (57) de Alba, E.; Blanco, F. J.; Jiménez, M. A.; Rico, M.; Nieto, J. L. *Eur. J. Biochem.* **1995**, *233*, 283–292.

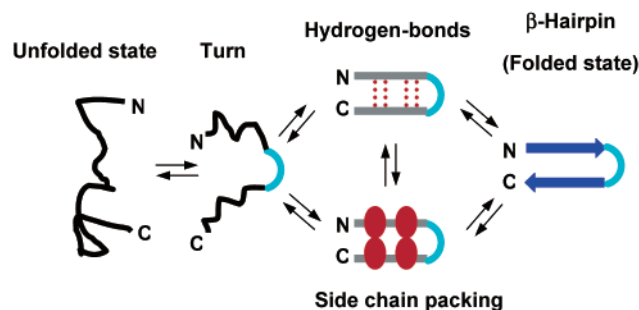


Figure 3. Model for  $\beta$ -hairpin folding.

It is true that the strict application of the two-state ( $\beta$ -hairpin-coil) model to the folding–unfolding equilibrium of linear  $\beta$ -hairpin peptides is questionable. A more rigorous treatment introducing several coupled intermediate states would be exceedingly complicated and most probably would lead to ambiguous results. However, it is evident that the  $\delta$  vs  $T$  curves provide an extraordinary wealth of information on the structure and energetics of the peptides. To take advantage of this information, we have approximated the complete folding–unfolding equilibrium as multistate processes consisting of consecutive “two-state” steps. This simplified model implies the existence of several intermediate states (three, in principle; see below) with increasing structure formed successively in the folding process. Following this approach, differences in the  $T_m$  values from distinct peptide regions can provide insight into the mechanism of  $\beta$ -hairpin folding. It is reasonable to assume that the regions in a peptide with the highest  $T_m$  values being the last ones to unfold, can, in turn, be the first ones to fold in the reverse process. This interpretation is equivalent to that commonly applied in proteins, where the differences in  $T_m$  values among denaturation curves obtained with different spectroscopic techniques, for example, fluorescence and CD in the far UV, are taken as evidence for the existence of an intermediate in protein unfolding–folding equilibrium. Stronger support to this assumption comes from recent results on cytochrome *c*<sup>58</sup> and ribonuclease HI,<sup>59</sup> whose folding pathways as established by kinetics measurements were found to be very similar if not the same as those derived from native-state hydrogen exchange, where the assumption that the last unfolded is equivalent to the first folded was also made.

Formation of a  $\beta$ -hairpin structure would include the following events: (i) turn formation, (ii) strand pairing by hydrogen-bonding formation, and (iii) strand pairing by side-chain packing, including cross-strand pairwise side chain interactions, formation of hydrophobic clusters, and hydrophobic surface burial. The order of these three events during folding, which would be cooperative and occur simultaneously in a “true” two-state transition, can be drawn from  $T_m$  values corresponding to protons in different  $\beta$ -hairpin regions of the six examined peptides. According to these data, we propose a multistep  $\beta$ -hairpin-folding model (Figure 3). This model is compatible with the presently available experimental data, from either our or other groups, on different  $\beta$ -hairpin systems. The first step is the formation of the turn, which mainly depends on local interactions. The bending of the peptide backbone would occur

in segments composed of residues with high  $\beta$ -turn propensities. Once formed, the turn promotes the coming together of the preceding and following peptide segments, so as to configure them as the N- and C-terminal strands that constitute the  $\beta$ -hairpin. The alignment of the strands will depend on which turn has been formed, and this “directed” alignment will be stabilized by hydrogen-bonding between the strands and by side chain–side chain interactions. These two stabilizing mechanisms can occur simultaneously (as in peptides 2, 3, and 5 in D<sub>2</sub>O; Table 3) or consecutively (as in peptides 4 and 6 in D<sub>2</sub>O; Table 3), where  $\beta$ -hairpin folding takes place in three steps. If the stabilization provided by the strands ( $\beta$ -sheet propensities, hydrogen bonds, and side-chain packing) is too weak, the  $\beta$ -hairpin will not form or will have a very low population within the conformational ensemble. This is the case for peptide 7 (Table 1), a 9-residue peptide,<sup>60</sup> and three Ala-containing variants of the 12-residue  $\beta$ -hairpin peptide designed by Ramírez-Alvarado et al.,<sup>44</sup> which form little or no  $\beta$ -hairpin, despite having turn sequences with strong propensities for forming turns. The absence of a sequence appropriate for the turn region will preclude  $\beta$ -hairpin formation, accounting for the complete  $\beta$ -hairpin destabilization observed in dPro-stabilized  $\beta$ -hairpins upon substituting dPro by LPro.<sup>52,53,61</sup> This shows that having a favorable turn sequence is necessary but not sufficient for a high population of  $\beta$ -hairpin. When two or more turns are formed in a peptide during the first step of the proposed mechanism, the corresponding two or more  $\beta$ -hairpins will be formed if the final stability provided by their strands is similar. The population of each  $\beta$ -hairpin is governed by its global stability, as shown by the case of peptides adopting two different  $\beta$ -hairpin structures.<sup>23–25</sup>

Peptide 5 in 30% TFE is the only clear exception to this model (Table 3), since the turn has a lower  $T_m$  than the strand structure. This result can be ascribed to the differential effects of this cosolvent<sup>41</sup> on the distinct contributions to  $\beta$ -hairpin stability, which can modify the energetic balance.

The proposed  $\beta$ -hairpin-folding mechanism is based on equilibrium data, so that it would be more appropriate to consider these results in terms of the unfolding energetics of each region, rather than as a kinetic sequence of events. A statistic mechanical model based on the only existing kinetics study on a  $\beta$ -hairpin peptide suggests that the turn region and the pairing of the adjacent residues are formed first;<sup>62,63</sup> this supports the idea that our model is also valid kinetically. Our model is also in agreement with a molecular dynamics simulation in which turn formation is the first stage in the  $\beta$ -hairpin folding.<sup>64</sup> It appears, however, to be in contrast with some other molecular dynamics simulations where the hydrophobic cluster occurs first in  $\beta$ -hairpin folding.<sup>65,66</sup> Even these cases could fit within our model, if turn formation is considered to be the bending of the peptide chain so as to facilitate hydrophobic

(60) Blanco, F. J.; Jiménez, M. A.; Herranz, J.; Rico, M.; Santoro, J.; Nieto, J. L. *J. Am. Chem. Soc.* **1993**, *115*, 5887–5888.

(61) Raghobama, S. R.; Awasthi, S. K.; Balam, P. *J. Chem. Soc., Perkin. Trans. 2* **1998**, 137–143.

(62) Muñoz, V.; Thompson, P. A.; Hofrichter, J.; Eaton, W. A. *Nature* **1997**, *390*, 196–199.

(63) Muñoz, V.; Henry, E. R.; Hofrichter, J.; Eaton, W. A. *Proc. Natl. Acad. Sci. U.S.A.* **1998**, *95*, 5872–5879.

(64) Bonvin, A. M.; van Gunsteren, W. F. *J. Mol. Biol.* **2000**, *296*, 255–268.

(65) Dinner, A. R.; Lazaridis, T.; Karplus, M. *Proc. Natl. Acad. Sci. U.S.A.* **1999**, *96*, 9068–9073.

(66) Pande, V. S.; Rokhsar, D. S. *Proc. Natl. Acad. Sci. U.S.A.* **1999**, *96*, 9062–9067.

(58) Hoang, L.; Bedard, S.; Krishna, M. M.; Lin, Y.; Englander, S. W. *Proc. Natl. Acad. Sci. U.S.A.* **2002**, *99*, 12173–12178.

(59) Spudich, G.; Lorenz, S.; Marqusee, S. *Protein Sci.* **2002**, *11*, 522–528.

clustering rather than the acquisition of a well-defined turn geometry.

### Conclusions

$^1\text{H}$  chemical shifts constitute extremely useful probes to investigate the unfolding of partially populated secondary structure conformations in linear peptides. According to the positive values of  $\Delta H_m$  and  $\Delta S_m$  for the thermal unfolding of  $\beta$ -hairpins, the formation of those structures is enthalpy-driven and entropy-unfavorable.  $T_m$  values are suitable to analyze the ability of different peptides to adopt  $\beta$ -hairpin structures. In the case of peptides **1–6**, this analysis reproduces the conclusions drawn by considering the  $\beta$ -hairpin populations estimated from  $\Delta\delta_{\text{C}\alpha\text{H}}$ ,  $\Delta\delta_{\text{C}\alpha}$ , and  $\Delta\delta_{\text{C}\beta}$  values.<sup>8,23–25,38</sup> Thus, the importance of the turn region for  $\beta$ -hairpin formation is evidenced once more, and the stabilizing effect of increasing the strand length previously shown only in dPro-containing peptides<sup>10</sup> is demonstrated in our peptide system. The differences in  $T_m$  obtained for protons belonging to different  $\beta$ -hairpin regions in a particular peptide (Table 3) indicate that  $\beta$ -hairpin unfolding is not a two-state transition.  $T_m$  can be considered to indicate the order of unfolding of the different  $\beta$ -hairpin regions, turn, strands, backbone, and side chains. Then, the existence of an order pattern shared by most of the peptides allows us to propose

a  $\beta$ -hairpin folding model in which the formation of the turn is the first event to take place.

**Supporting Information Available:** A brief description of the NMR study of peptide **2** in 2 M NaCl and in 2 M Gly, including Figure SM1, which contains the  $\text{C}\alpha\text{H}$  conformational shifts as a function of sequence; Tables SM1 and SM2, listing the  $^1\text{H}$   $\delta$  values of peptide **2** in aqueous solution in 2 M NaCl and in 2 M Gly, respectively; and Tables SM3–SM12, listing the  $\Delta\delta_{(T_{\text{low}}-T_{\text{high}})}$  for peptides **1–7** in  $\text{D}_2\text{O}$ , as well as for peptide **2** in 2 M NaCl and in 2 M Gly and for peptide **5** in 30% TFE. This material is available free of charge via the Internet at <http://pubs.acs.org>.

**Acknowledgment.** We thank Mrs. C. López and Mr. L. de la Vega for technical assistance and Dr. D. V. Laurents for revising the English in the manuscript. We also appreciate helpful discussions with Prof. N. H. Andersen at the earliest stage of our thermodynamic analyses. This work was supported by the Spanish DGYCT project no. PB98-0677 and European project no. CEE B104-97-2086. C.M.S. is a recipient of a predoctoral fellowship from the Autonomous Community of Madrid, Spain.

JA0278537